MORPHOLOGICAL AND OPTICAL INVESTIGATION OF CuO FIBERS PREPARED VIA ELECTROSPINNING

Cristina BUSUIOC[1], Vasile-Adrian SURDU[2], Ecaterina ANDRONESCU[3]

The objective of the paper was the synthesis and characterization of CuO nanofibers. These were obtained by electrospinning a solution of copper (II) acetate monohydrate and polyvinylpyrrolidone in N,N-dimethylformamide, followed by calcination at 400, 450, 500 or 600 °C for 2 or 8 h. The compositional, structural, morphological and optical properties of the resulting fibers were investigated by X-ray diffraction, scanning electron microscopy and reflectance spectroscopy. The thermally treated samples exhibit CuO unique phase with polycrystalline monoclinic structure. SEM analysis revealed a five times decrease of fiber diameter after calcination, as well as a fiber porosity reduction with calcination temperature increasing. The optical studies led to band gap values of 1.36 ± 0.01 eV.

Keywords: CuO, semiconductor, nanofibers, electrospinning, bang gap

1. Introduction

One-dimensional (*1D*) semiconducting nanostructures such as nanofibers, nanotubes, nanowires and nanorods have attracted growing interest in the recent years due to their unique optical and/or electrical properties, which make them suitable for applications in the field of electronics, optoelectronics, catalysis, solar cells and biological or chemical sensors [1-3]. In this context, a wide range of transition metal oxides (CuO, ZnO, TiO_2, WO_3 etc.) have been obtained in the form of *1D* nanomaterials by various techniques [4-6]. Compared with their micro or bulk counterparts, these nanostructures exhibit high surface-to-volume ratio, modified surface energy and potential size effects, which lead to interesting chemical and physical properties and promising applications in many fields [7].

Copper oxide (CuO) is a well known *p*-type semiconductor with a narrow direct band gap (1.2 eV in bulk) [8]. Most of the properties of CuO depend on its morphology [7], as a consequence, the researchers developed many methods for the synthesis of CuO nanostructures [9-16], which are good candidates for

[1] PostDoc researcher, Dept. of Science and Engineering of Oxide Materials and Nanomaterials, University POLITEHNICA of Bucharest, National Institute of Materials Physics, Bucharest, Romania, e-mail: jinga_cristina@yahoo.co.uk, cristina.busuioc@infim.ro

[2] Graduate student, Dept. of Science and Engineering of Oxide Materials and Nanomaterials, University POLITEHNICA of Bucharest, Romania, e-mail: adrian.surdu@live.com

[3] Prof., Dept. of Science and Engineering of Oxide Materials and Nanomaterials, University POLITEHNICA of Bucharest, Romania, e-mail: ecaterina.andronescu@upb.ro

applications like gas sensors, photocatalysts, field effect transistors, solar cells, lithium ion batteries, photodetectors, supercapacitors etc. [2, 7, 17-19].

Electrospinning or electrostatic field-assisted fiber deposition is a simple and inexpensive method used for the synthesis of polymer, metallic and ceramic fibers with diameters ranging from tens of nanometers to several micrometers [20]. This technique involves the preparation of a precursor solution, which is pumped at a constant rate under a high electric field, the resulting fiber being gathered on a collector that is placed at a certain distance from the pumping system; the method yields fibers in the form of a nonwoven mesh if the collector is stationary and in the form of well-aligned arrays when using a rotating collector.

Most of the papers on electrospun CuO fibers reported on using cupric acetate and polyvinyl alcohol as starting materials and calcination temperatures greater than or equal to 500 °C combined with long calcination times [21-23]. Wang *et al.* [24] used polyacrylonitrile as carrier polymer for the synthesis of hollow CuO particles via electrospinning method and developed a sensitive nonenzymatic hydrogen peroxide sensor based on the mentioned structures. *1D* metal oxide nanomaterials have a great potential in biological or chemical sensing due to their large surface-to-volume ratio. In this context, Choi *et al.* [21] studied the growth behavior of nanograins in CuO nanofibers synthesized by electrospinning and showed that larger nanograins lead to a much higher sensitivity of the corresponding gas sensors in terms of CO and NO_2. Moreover, Wang *et al.* [22] fabricated enzymeless glucose sensors using three-dimensional network films of electrospun CuO nanofibers and demonstrated its superiority towards electrode fouling to glucose detection. Sahay *et al.* [23] obtained highly crystalline CuO nanofibers using the electrospinning technique and investigated the catalytic activity of these nanostructures for the degradation of methyl orange, as well as their suitability as blocking layer in ZnO-based dye sensitized solar cell, configuring possible energy applications.

In this work, the electrospinning technique was used for the fabrication of CuO fibers. The precursor composite fibers were calcined at temperatures in the 400 - 600 °C range for different times. Polyvinylpyrrolidone was used for the first time as carrier polymer for the preparation of CuO fibers, this representing the novelty of our work. Furthermore, the influence of the processing parameters on the properties of the resulting fibers was studied.

2. Experimental procedure

CuO fibers were prepared by the electrospinning technique. Copper (II) acetate monohydrate ($Cu(Ac)_2 \cdot H_2O$, Sigma-Aldrich, ≥99%) was used as source of metallic cations, polyvinylpyrrolidone (PVP, MW = 1.300.000, Sigma-Aldrich) as

carrier polymer and N,N-dimethylformamide (DMF, ≥99,8%, Sigma-Aldrich) as solvent. First, 0.5 g of $Cu(Ac)_2 \cdot H_2O$ was dissolved in 5 mL DMF with stirring for 2 h at 50 °C. Then, 1 g of PVP was added, the resulting solution being stirred for 10 h at 50 °C. A dark green solution was obtained. Further, the precursor solution was loaded in a plastic syringe with a blunt tipped stainless needle (0.8 mm interior diameter), which was connected to a syringe pump set to a feeding rate of 0.1 mL/h. A positive voltage of 25 kV was applied to the needle, the metal collector being grounded and placed at a distance of 20 cm from the tip of the needle. Silicon plates were employed as substrates. The schematic representation of the experimental setup is displayed in Fig. 1. In order to obtain single phase crystalline CuO fibers, the as-spun hybrid fibers were calcined in a convection oven for 2 or 8 h at 400, 450, 500 or 600 °C, in air.

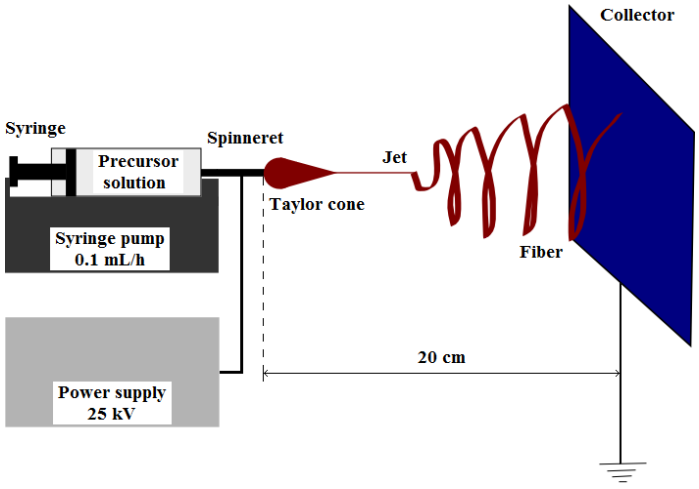

Fig. 1. Illustration of the electrospinning setup.

CuO fibers were investigated by thermal analysis (DTA-TG), X-ray diffraction (XRD), scanning electron microscopy (SEM) and reflectance spectroscopy (RS). The thermal analysis was performed on a Shimadzu DTG-60 equipment, in the 20 - 600 °C temperature range, in air. A PANalytical Empyrean diffractometer with Cu Kα radiation (λ = 0.154 nm), equipped with a Hybrid monochromator 2xGe(220) for Cu and parallel plate collimator mounted on PIXcel3D detector was used to identify the crystalline phases and structure of the calcined fibers; 2θ was ranged between 20 and 80 °, while the incidence angle was set at 0.5 °. The microstructure of the precursor and CuO fibers was analyzed with an Zeiss Evo 50 XVP scanning electron microscope. The reflectance spectra were recorded with a Perkin Elmer Lambda 45 UV-Vis spectrophotometer equipped with an integrating sphere.

3. Results and discussion

The thermal analysis of the as-spun hybrid fibers is presented in Fig. 2. The thermogravimetric data show three major weight loss steps in the 20 - 270 °C temperature range, corresponding to a weight loss of more than 95%. The mentioned value is higher than the theoretical one (around 75%), meaning that part of the resulting CuO fibers (fluffy and porous fibers) are carried off the balance by the air flow. The first minor endothermic effect below 100 °C is assigned to the evaporation of the residual solvent and loss of moisture or other adsorbed molecules. The second small effect is an exothermic one and corresponds to the intramolecular degradation of PVP. The strong exothermic effect with maximum at 250 ° is attributed to the intermolecular degradation of PVP and $CuAc_2 \cdot H_2O$ decomposition, with CuO crystallisation. It is obvious that all volatile matters and organic components are completely removed below 270 °C, which leads to the conclusion that the existence of Cu^{2+} ions decreases the decomposition temperature of PVP, indicating the existence of some interaction between PVP and the metal ions [25].

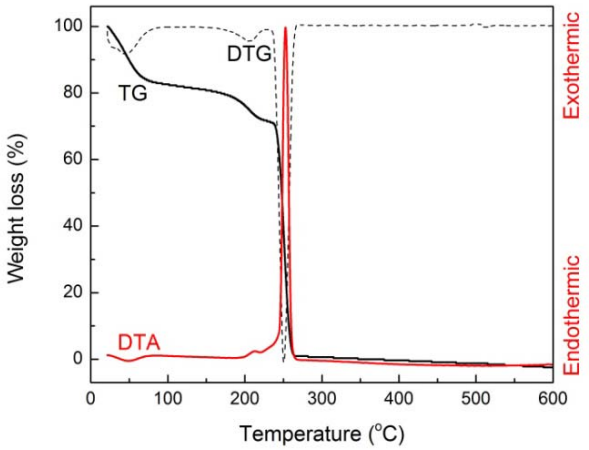

Fig. 2. Thermal analysis of the precursor fibers.

The phase composition and crystal structure of the thermally treated fibers were investigated by XRD. Fig. 3 shows the X-ray diffractograms of CuO fibers calcined at three different temperatures. The diffraction peaks placed at 2θ: 32.5, 35.5, 38.7, 46.2, 48.7, 53.4, 58.3, 61.5, 66.2, 68.1, 72.3 and 75.2 were assigned to the following crystal planes: (110), (002)/(-111), (111)/(200), (-112), (-202), (020), (202), (-113), (022)/(-311), (113)/(220), (311) and (004)/(-222), indicating the formation of the monoclinic CuO phase (JCPDS 04-009-2287) with high

crystallinity. Further, the average crystallite size was estimated by using the Scherrer equation: $D=K\cdot\lambda/(\beta\cdot\cos\theta)$, where K is a dimensionless shape factor with a typical value of about 0.9, λ is the X-ray wavelength (0.154 nm), β is the full width at half maximum value and θ is the Bragg angle. As expected, the increase of the calcination temperature leads to larger crystallites, the resulting values being 20 nm (400 °C / 8h), 26 nm (450 °C / 2h) and 29 nm (500 °C / 2h), respectively.

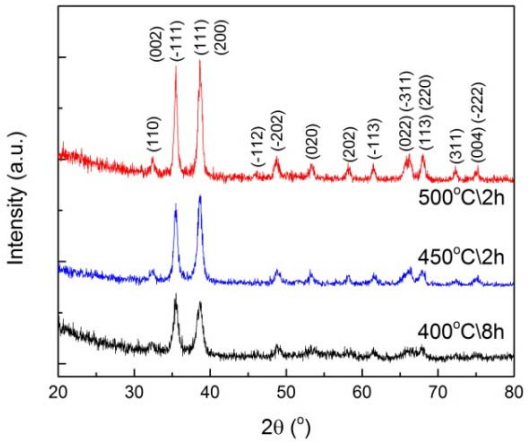

Fig. 3. XRD patterns of CuO fibers calcined at different temperatures.

Further, the morphology of CuO fibers obtained by electrospinning was examined by SEM. Fig. 4 presents SEM images of the as-spun hybrid fibers, as well as CuO fibers calcined at different temperatures. The precursor fibers are continuous, with smooth surface and exhibit diameter values in the 300 - 500 nm range (Fig. 4a). The thermal treatment enables acetate and PVP decomposition, as well as CuO formation, but also modifies the overall aspect of the fibers. Thus, the diameter is reduced to values placed in the 50 - 100 nm range (Fig 4b-e), about five times lower than before calcinations. Moreover, the surface of the fibers becomes rough and some of them break due to the contraction that occurs during the thermal treatment. This breaking tendency accentuates with calcination temperature increasing, so that the sample calcinated at 600 °C / 8h consists of disparate particles (Fig. 4f). The phenomenon of fiber disintegration is driven by the so-called Rayleigh instability [26]. Regarding the fiber porosity, it can be stated that the increase of the calcination temperature or time determines a decrease in porosity, the sample calcined at 500 °C / 8h displaying the highest densification. As it was expected and already proved by the XRD analysis, the average size of the individual particles that compose the fibers increases with

calcination temperature or time increasing. In this context, CuO fibers with high porosity can be used for applications in the field of catalysis, while those with low porosity can be integrated in field effect transistors or sensors.

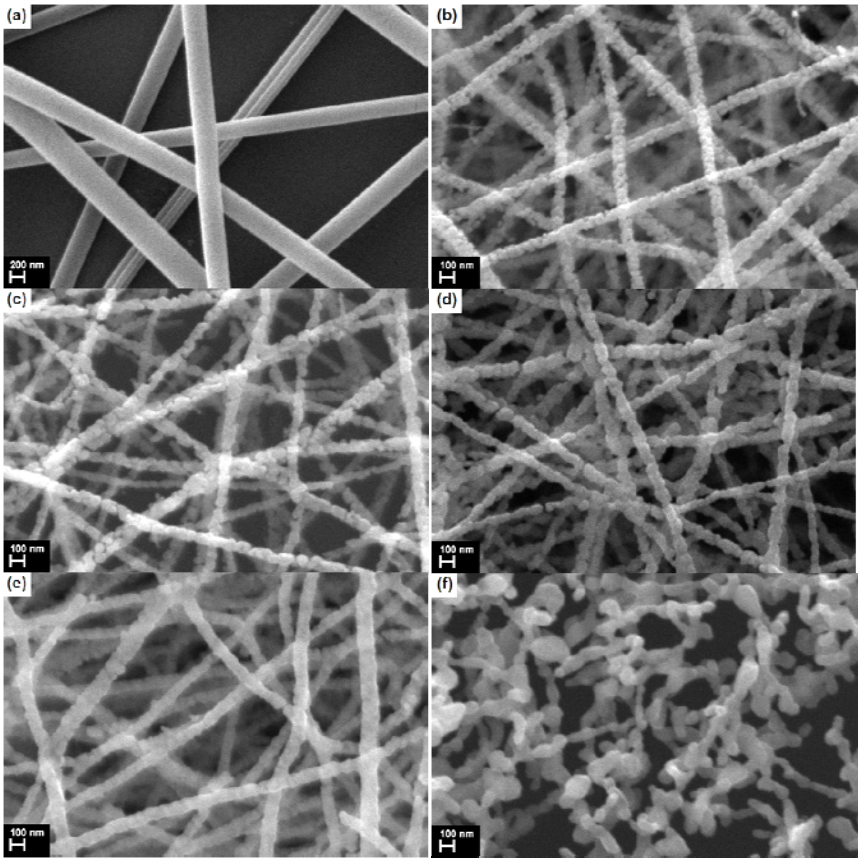

Fig. 4. SEM images of the precursor fibers (a) and CuO fibers calcined at 400 °C / 8 h (b), 450 °C / 2 h (c), 500 °C / 2 h (d), 500 °C / 8 h (e) and 600 °C / 8 h (f).

The optical properties of CuO fibers were also investigated, Fig. 5a showing the reflection spectra of all prepared samples. The pronounced decrease of the reflectance between 885 and 895 nm is assigned to the band-to-band transition in CuO. In order to estimate the band gap values, Kubelka-Munk functions ($F(R)$) were calculated and $[F(R)\cdot E]^{1/2}$ functions were plotted versus photon energy (E) (Fig. 5b).

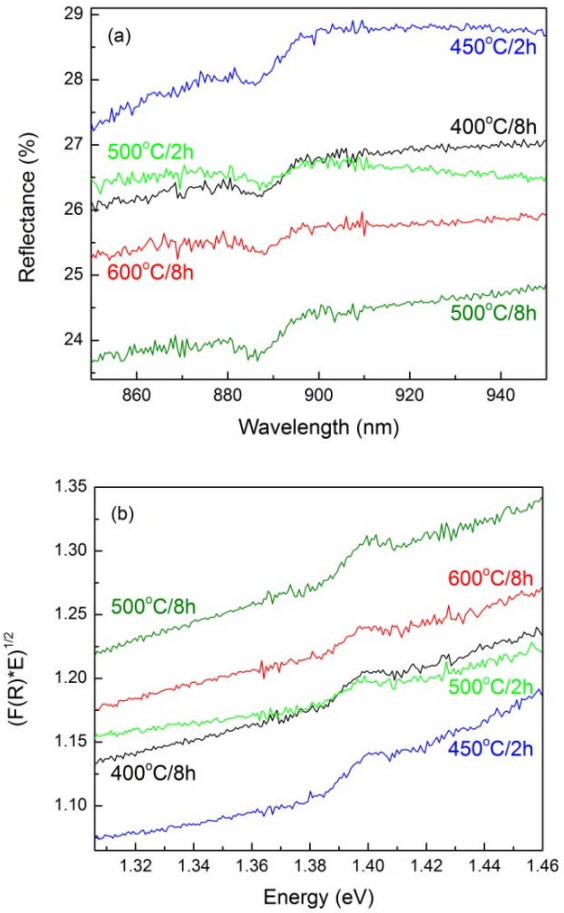

Fig. 5. Reflectance spectra (a) and representation of Kubelka-Munk functions (b) for CuO fibers.

Kubelka-Munk function is expressed as $F(R)=(1-R)^2/(2\cdot R)$, where R is the observed diffuse reflectance. The resulting band gap values are 1.36 ± 0.01 eV. The blue-shift in the band gap energy of CuO nanofibers can be a result of the quantum confinement from bulk CuO (1.2 eV) to *1D* nanostructures [23].

4. Conclusions

CuO nanofibers were successfully prepared by the electrospinning technique. The precursor composite fibers were calcined in different conditions (temperatures between 400 and 600 °C and times of 2 or 8 h) in order to provide polymer burning and CuO crystallisation in monoclinic phase. The resulting fibers exhibit diameter values below 100 nm, five times lower than before the thermal

treatment. The increase of the calcination temperature leads to crystallite size increase, as well as fiber porosity decrease. All samples present band gap values of 1.36 ± 0.01 eV, showing that the processing conditions do not influence the optical properties. Such thin semiconducting fibers prepared by a straightforward approach can be used for applications in the field of catalysts, field effect transistors or sensors.

Acknowledgments

The work has been funded by the Sectoral Operational Programme Human Resources Development 2007-2013 of the Ministry of European Funds through the Financial Agreement POSDRU/159/1.5/S/132397.

R E F E R E N C E S

[1] *F. Rahman*, Nanostructures in Electronics and Photonics, Pan Stanford Publishing, Singapore, 2008.

[2] *S. Zaman*, Synthesis of ZnO, CuO and Their Composite Nanostructures for Optoelectronics, Sensing and Catalytic Applications, LiU-Tryck, Linkoping, 2012.

[3] *P.C. Chen, G. Shen, C. Zhou*, Chemical Sensors and Electronic Noses Based on 1-D Metal Oxide Nanostructures, IEEE Transactions on Nanotechnology 7 [6] 668–682 (2008).

[4] *M. Lugo-Ruelas, P. Amézaga-Madrid, O. Esquivel-Pereyra, W. Antúnez-Flores, P. Pizá-Ruiz, C. Ornelas-Gutiérrez, M. Miki-Yoshida*, Synthesis, Microstructural Characterization and Optical Properties of CuO Nanorods and Nanowires Obtained by Aerosol Assisted CVD, Journal of Alloys and Compounds doi:10.1016/j.jallcom.2014.11.119.

[5] *S. Wei, S. Wang, Y. Zhang, M. Zhou*, Different Morphologies of ZnO and Their Ethanol Sensing Property, Sensors and Actuators B 192 (2014) 480–487.

[6] *D. Portan, K. Papaefthymiou, C. Pîrvu, G. Papanicolaou, I. Demetrescu*, Manufaturing and Characterization of TiO_2 Nanotubes on Pure Titanium Surface for Advanced Biomedical Applications, University Politehnica of Bucharest Scientific Bulletin Series B 73 [2] 181–196 (2011).

[7] *Q. Zhang, K. Zhang, D. Xu, G. Yang, H. Huang, F. Nie, C. Liu, S. Yang*, CuO Nanostructures: Synthesis, Characterization, Growth Mechanisms, Fundamental Properties, and Applications, Progress in Materials Science 60 (2014) 208–337.

[8] *H.J. Kim, J.H. Lee*, Highly Sensitive and Selective Gas Sensors Using p-Type Oxide Semiconductors: Overview, Sensors and Actuators B 192 (2014) 607–627.

[9] *P. Gao, Y. Chen, H. Lv, X. Li, Y. Wang, Q. Zhang*, Synthesis of CuO Nanoribbon Arrays with Noticeable Electrochemical Hydrogen Storage Ability by a Simple Precursor Dehydration Route at Lower Temperature, International Journal of Hydrogen Energy 34 (2009) 3065–3069.

[10] *W. Gao, S. Yang, S. Yang, L. Lv, Y. Du*, Synthesis and Magnetic Properties of Mn Doped CuO Nanowires, Physics Letters A 375 (2010) 180–182.

[11] *S.E. Moosavifard, J. Shamsi, S. Fani, S. Kadkhodazade*, Facile Synthesis of Hierarchical CuO Nanorod Arrays on Carbon Nanofibers for High-Performance Supercapacitors, Ceramics International 40 (2014) 15973–15979.

[12] *R.M. Mohameda, F.A. Harrazb, A. Shawkyb*, CuO Nanobelts Synthesized by a Template-Free Hydrothermal Approach with Optical and Magnetic Characteristics, Ceramics International 40 (2014) 2127–2133.

[13] *J.G. Zhao, J.Z. Yin, M. Yang*, Hydrothermal Synthesis and Magnetic Properties of CuO Hollow Microspheres, Materials Research Bulletin 49 (2014) 83–87.

[14] *H. Siddiqui, M.S. Qureshi, F.Z. Haque*, One-Step, Template-Free Hydrothermal Synthesis of CuO Tetrapods, Optik 125 (2014) 4663–4667.

[15] *H.J. Park, N.J. Choi, H. Kang, M.Y. Jung, J.W. Park, K.H. Park, D.S. Lee*, A ppb-Level Formaldehyde Gas Sensor Based on CuO Nanocubes Prepared Using a Polyol Process, Sensors and Actuators B 203 (2014) 282–288.

[16] *C. Yang, J. Wang, F. Xiao, X. Su*, Microwave Hydrothermal Disassembly for Evolution from CuO Dendrites to Nanosheets and Their Applications in Catalysis and Photo-Catalysis, Powder Technology 264 (2014) 36–42.

[17] *Q. Wang, J. Zhao, W. Shan, X. Xia, L. Xing, X. Xue*, CuO Nanorods/Graphene Nanocomposites for High-Performance Lithium-Ion Battery Anodes, Journal of Alloys and Compounds 590 (2014) 424–427.

[18] *S.B. Wang, C.H. Hsiao, S.J. Chang, K.T. Lam, K.H. Wen, S.C. Hung, S.J. Young, B.R. Huang*, A CuO Nanowire Infrared Photodetector, Sensors and Actuators A: Physical 171 (2011) 207–211.

[19] *M. Huang, F. Li, Y.X. Zhang, B. Li, X. Gao*, Hierarchical NiO Nanoflake Coated CuO Flower Core-Shell Nanostructures for Supercapacitor, Ceramics International 40 (2014) 5533–5538.

[20] *S. Ramakrishna, K. Fujihara, W.E. Teo, T.C. Lim, Z. Ma*, An Introduction to Electrospinning and Nanofibers, World Scientific Publishing, Singapore, 2005.

[21] *S.W. Choi, J.Y. Park, S.S. Kim*, Growth Behavior and Sensing Properties of Nanograins in CuO Nanofibers, Chemical Engineering Journal 172 (2011) 550–556.

[22] *B. Wang, L. Luo, Y. Ding, D. Zhao, Q. Zhang*, Synthesis of Hollow Copper Oxide by Electrospinning and Its Application as a Nonenzymatic Hydrogen Peroxide Sensor, Colloids and Surfaces B: Biointerfaces 97 (2012) 51–56.

[23] *R. Sahay, J. Sundaramurthy, P. Suresh Kumar, V. Thavasi, S.G. Mhaisalkar, S. Ramakrishna*, Synthesis and Characterization of CuO Nanofibers, and Investigation for Its Suitability as Blocking Layer in ZnO NPs Based Dye Sensitized Solar Cell and as Photocatalyst in Organic Dye Degradation, Journal of Solid State Chemistry 186 (2012) 261–267.

[24] *W. Wang, L. Zhang, S. Tong, X. Li, W. Song*, Three-Dimensional Network Films of Electrospun Copper Oxide Nanofibers for Glucose Determination, Biosensors and Bioelectronics 25 (2009) 708–714.

[25] *W. Wang, Z. Feng, W. Jiang, J. Zhan*, Electrospun Porous CuO–Ag Nanofibers for Quantitative Sensitive SERS Detection, CrystEngComm 15 (2013) 1339–1344.

[26] *P.W. Fan, W.L. Chen, T.H. Lee, Y.J. Chiu, J.T. Chen*, Rayleigh-Instability-Driven Morphology Transformation by Thermally Annealing Electrospun Polymer Fibers on Substrates, Macromolecules 45 (2012) 5816.